

Synthesis and Magnetic Property of Copper(II)–Lanthanide(III) Complexes $[\{Cu^{II}LLn^{III}(o\text{-van})(CH_3COO)(MeOH)\}_2]\cdot 2H_2O$ (Ln^{III} = Gd^{III}, Tb^{III}, and Dy^{III}; H_3L = 1-(2-Hydroxybenzamido)-2-(2-hydroxy-3-methoxybenzylideneamino)ethane; *o*-van = 3-Methoxysalicylaldehydato)

Takefumi Hamamatsu,[1] Kazuya Yabe,[1] Masaaki Towatari,[1] Naohide Matsumoto,*[1] Nazzareno Re,[2] Andrzej Pochaba,[3] and Jerzy Mrozinski[3]

[1]Department of Chemistry, Faculty of Science, Kumamoto University, 2-39-1 Kurokami, Kumamoto 860-8555

[2]Faculty of Pharmacy, Università degli Studi "G. D'Annunzio," I-66100 Chieti, Italy

[3]Faculty of Chemistry, University of Wroclaw, 14 F. Joliot-Curie, 50-383 Wroclaw, Poland

Received September 6, 2006; E-mail: naohide@aster.sci.kumamoto-u.ac.jp

Three tetranuclear copper(II)–lanthanide(III) complexes, $[\{Cu^{II}LLn^{III}(o\text{-van})(CH_3COO)(MeOH)\}_2]\cdot 2H_2O$ (Ln^{III} = Gd^{III}, Tb^{III}, and Dy^{III}), were synthesized and characterized, where H_3L is 1-(2-hydroxybenzamido)-2-(2-hydroxy-3-methoxybenzylideneamino)ethane and *o*-van is 3-methoxysalicylaldehydato. These compounds are isomorphous to each other and consist of a cyclic tetranuclear $Cu^{II}{}_2Ln^{III}{}_2$ structure, in which the Cu^{II} and Ln^{III} ions are alternately arrayed and the Cu^{II} component complex. $[Cu^{II}L]^-$ unit functions as a "bridging ligand-complex" between two adjacent Ln^{III} ions through the phenolato and methoxy oxygen atoms at one side and the amido oxygen atom at the another side. The temperature-dependent magnetic susceptibilities from 2.0 to 300.0 K and the field-dependent magnetizations at 2.0 K from 0 to 5 T showed that the magnetic interaction between Cu^{II} and each of the lanthanide ions is ferromagnetic. The magnetic susceptibilities of $[\{Cu^{II}LGd^{III}(o\text{-van})(CH_3COO)(MeOH)\}_2]\cdot 2H_2O$ were analyzed by using a spin-only Hamiltonian $\boldsymbol{H} = -2J_1(S_{Cu1}S_{Gd1} + S_{Cu2}S_{Gd2}) - 2J_2(S_{Cu1}S_{Gd2} + S_{Cu2}S_{Gd1})$ based on a cyclic tetranuclear structure and gave the best-fit parameters of $g = 1.97$, $J_1 = +3.8\,cm^{-1}$, $J_2 = +0.7\,cm^{-1}$, and $zJ' = -0.01\,cm^{-1}$. The magnetization data at 2.0 K of $[\{Cu^{II}LGd^{III}(o\text{-van})(CH_3COO)(MeOH)\}_2]\cdot 2H_2O$ were well reproduced by using a Brillouin function with an $S = 8$ spin ground state due to the ferromagnetic interactions between Cu^{II} and Gd^{III} ions and $g = 1.97$. The ac magnetic susceptibilities of $[\{Cu^{II}LLn^{III}(o\text{-van})(CH_3COO)(MeOH)\}_2]\cdot 2H_2O$ (Ln^{III} = Tb^{III} and Dy^{III}) in the temperature range 1.8–10.0 K with a 3 G ac field oscillating in the range 1–1000 Hz showed a frequency dependence characteristic of SMMs.

Single molecule magnets (SMMs) have attracted special attention in the past decade, since each individual molecule of a SMM can function as a nanoscale magnet.[1] A SMM exhibits not only the classical properties of a magnet, but also straddles the classical/quantum interface, such as the quantum tunneling of magnetization. Since the first discovery of SMM in the Mn_{12} cluster, studies have been focused on 3d clusters, and a number of SMMs have been found in Mn, Fe, V, Ni, and hetero-metal 3d clusters.[1] On the basis of the theoretical and experimental studies, it is now well established that to be SMMs molecules must have a high-spin ground state and large easy-axis type magnetic anisotropy.[2] The unusual combination of high-spin ground state and magnetic anisotropy gives a magnetic bistable molecule, resulting in a significant barrier to thermally activated magnetization relaxation.

Since the conditions for SMMs, i.e., high-spin ground state and magnetic anisotropy, are not easily achieved and the blocking temperatures (T_B) of the SMMs so far reported are still limited to around liquid helium temperature,[1,2] fundamentally new synthetic designs for SMMs are required. Ishikawa's group reported that Tb^{III}, Dy^{III}, and Ho^{III} phthalocyanines exhibit SMM behavior, and even mononuclear 4f molecule can be SMMs.[3] We have reported the first 3d–4f SMMs exhibiting frequency dependent out-of-phase ac signals, $[\{Cu^{II}LTb^{III}(hfac)_2\}_2]$ and $[\{Cu^{II}LDy^{III}(hfac)_2\}_2]$ (H_3L = 1-(2-hydroxybenzamido)-2-(2-hydroxy-3-methoxybenzylideneamino)ethane and Hhfac = hexafluoroacetylacetone), in which the compounds have a cyclic tetranuclear $Cu^{II}{}_2Ln^{III}{}_2$ structure.[4] There are several advantages with these 3d–4f SMMs: (1) the magnetic vectors of the adjacent 3d and 4f ions can be simply assembled due to the cyclic structure, and a high-spin ground state can be obtained by the ferromagnetic coupling between Cu^{II} and Ln^{III} ions (ferromagnetic coupling is observed for the combinations of Cu^{II}–Gd^{III}, Cu^{II}–Tb^{III}, and Cu^{II}–Dy^{III}), (2) a high-spin ground state can be obtained with a smaller number of metal ions than in 3d clusters, and (3) molecular magnetic anisotropy is easily derived from the 4f-component, such as Tb^{III} and Dy^{III} ions. In recent years, the molecular design of SMMs and single-chain magnets (SCMs) containing f-block elements have attracted much attention.[5–12] Christou's

Published on the web March 13, 2007; doi:10.1246/bcsj.80.523

Table 1. X-ray Crystallographic Data for $[\{Cu^{II}LLn^{III}(o\text{-van})(CH_3COO)(MeOH)\}_2]\cdot 2H_2O$ (Ln^{III} = Gd^{III}, Tb^{III}, and Dy^{III})

	$Cu^{II}{}_2$–$Gd^{III}{}_2$	$Cu^{II}{}_2$–$Tb^{III}{}_2$	$Cu^{II}{}_2$–$Dy^{III}{}_2$
Formula	$C_{56}H_{62}N_4O_{22}Cu_2Gd_2$	$C_{56}H_{62}N_4O_{22}Cu_2Tb_2$	$C_{56}H_{62}N_4O_{22}Cu_2Dy_2$
Temp/K	296	296	296
Fw	1584.71	1588.06	1595.21
Space group	$P2_1/c$ (No. 14)	$P2_1/c$ (No. 14)	$P2_1/c$ (No. 14)
a/Å	12.167(4)	12.276(4)	12.092(5)
b/Å	14.085(6)	14.133(4)	14.021(5)
c/Å	16.026(6)	16.193(5)	16.093(5)
β/deg	95.42(1)	95.51(1)	96.07(1)
V/Å^3	2734(1)	2796(1)	2713(1)
Z	2	2	2
D_{calcd}/g cm^{-3}	1.925	1.886	1.952
μ/cm^{-1}	32.57	33.30	35.89
R, R_w	0.043, 0.139	0.048, 0.124	0.053, 0.173

group[5] and Pecoraro's group[6] have synthesized Mn^{III}–Dy^{III} clusters by original molecular designs and reported their SMMs properties. The $[Mn^{III}{}_{11}Dy^{III}{}_4]$ and $[Mn^{III}{}_2Dy^{III}{}_2]$ clusters reported by Christou's group[5] exhibit temperature and sweep rate dependent hysteresis loops. In addition, several reports on $[Cu^{II}Tb^{III}]$,[7] $[Cu^{II}{}_2Tb^{III}{}_2]$,[7] $[Cu^{II}Tb^{III}{}_4]$,[8] $[Cu^{II}{}_6Dy^{III}{}_3]$,[9] $[Fe^{III}Dy^{III}]$,[10] and $[Ni^{II}Ln^{III}]$,[11] have appeared recently. These complexes show frequency-dependent out-of-phase ac signals, demonstrating that the 3d–4f cluster approach is a very promising pathway to SMMs.

In this study, we modified the first 3d–4f SMMs, $[\{Cu^{II}LLn^{III}(hfac)_2\}_2]$ (Ln^{III} = Tb^{III} and Dy^{III}),[3] and synthesized three copper(II)–lanthanide(III) complexes $[\{Cu^{II}LLn^{III}(o\text{-van})(CH_3COO)(MeOH)\}_2]\cdot 2H_2O$ (Ln^{III} = Gd^{III}, Tb^{III}, and Dy^{III}), in which *o*-vanillin (3-methoxysalicylaldehyde) and acetate, instead of two hexafluoroacetylacetones, coordinate to the Ln^{III} ion as the terminal ligands. This study may answer the following questions: (1) "Are the Cu^{II}–Tb^{III} and Cu^{II}–Dy^{III} combinations always good combinations for SMMs of 3d–4f cluster?" and (2) "Can ligand substitution at the Ln^{III} terminal site give good quality of crystals and effectively increase the blocking temperature?"

Results and Discussion

Synthesis of $[\{Cu^{II}LLn^{III}(o\text{-van})(CH_3COO)(MeOH)\}_2]\cdot 2H_2O$ (Ln^{III} = Gd^{III}, Tb^{III}, and Dy^{III}). The component Cu^{II} complex $K[Cu^{II}L]\cdot MeOH$ with a tetradentate N_2O_2 ligand that is the 1:1:1 condensation product of *o*-vanillin (3-methoxysalicylaldehyde), ethylenediamine, and 2-hydroxybenzamide, was used for a "bridging ligand-complex."[13] Three copper(II)–lanthanide(III) complexes, $[\{Cu^{II}LLn^{III}(o\text{-van})(CH_3COO)_2(MeOH)\}_2]\cdot 2H_2O$ (Ln^{III} = Gd^{III}, Tb^{III}, and Dy^{III}), were prepared almost quantitatively by mixing $K[Cu^{II}L]\cdot MeOH$, $Ln^{III}(CH_3COO)_3\cdot 4H_2O$ (Ln^{III} = Gd^{III}, Tb^{III}, and Dy^{III}), and *o*-vanillin with the molar ratio of 1:1:1 in a mixed solution of *N*,*N*′-dimethylformamide (DMF) and methanol (1/4 volume) at ambient temperature. These complexes were easily obtained as crystals using diffusion method and used for all the physical measurements including elemental analyses, infrared spectroscopy, X-ray analyses, and magnetic measurements. Due to the use of *o*-vanillin, large crystals of $[\{Cu^{II}LLn^{III}(o\text{-van})(CH_3COO)_2(MeOH)\}_2]\cdot 2H_2O$ were obtained easier than those of $[\{Cu^{II}LLn^{III}(hfac)_2\}_2]$.

Table 2. Relevant Distances (Å) for $[\{Cu^{II}LLn^{III}(o\text{-van})(CH_3COO)(MeOH)\}_2]\cdot 2H_2O$ (Ln^{III} = Gd^{III}, Tb^{III}, and Dy^{III})[a)]

	$Cu^{II}{}_2$–$Gd^{III}{}_2$	$Cu^{II}{}_2$–$Tb^{III}{}_2$	$Cu^{II}{}_2$–$Dy^{III}{}_2$
Cu–Cu*	5.2388(9)	5.161(2)	5.2065(7)
Cu–Ln	5.7342(7)	5.696(1)	5.7065(5)
Cu–Ln*	3.4138(8)	3.412(1)	3.3813(5)
Ln–Ln*	7.8502(4)	7.8457(7)	7.8031(2)
Ln–O(1)	2.280(5)	2.285(6)	2.262(3)
Ln*–O(2)	2.430(4)	2.454(5)	2.406(2)
Ln*–O(3)	2.367(4)	2.358(7)	2.326(3)
Ln*–O(4)	2.580(4)	2.610(7)	2.553(3)
Ln–O(5)	2.398(5)	2.391(7)	2.351(4)
Ln–O(6)	2.283(6)	2.249(7)	2.249(4)
Ln–O(8)	2.470(4)	2.469(8)	2.447(3)
Ln–O(9)	2.441(4)	2.417(8)	2.412(3)
Cu–O(2)	1.922(4)	1.915(6)	1.929(3)
Cu–O(3)	1.948(4)	1.951(7)	1.947(2)
Cu–O(10)	2.515(5)	2.62(1)	2.494(3)
Cu–N(1)	1.917(5)	1.905(7)	1.921(3)
Cu–N(2)	1.950(6)	1.928(8)	1.933(3)

a) The asterisk denotes the symmetry operation of $-x$, $-y$, $-z$.

Structural Description of $[\{Cu^{II}LLn^{III}(o\text{-van})(CH_3COO)(MeOH)\}_2]\cdot 2H_2O$ (Ln^{III} = Gd^{III}, Tb^{III}, and Dy^{III}). Using diffusion method, the compounds $[\{Cu^{II}LLn^{III}(o\text{-van})(CH_3COO)(MeOH)\}_2]\cdot 2H_2O$ (Ln^{III} = Gd^{III}, Tb^{III}, and Dy^{III}) were easily obtained as block crystals suitable for the single-crystal X-ray analyses. Crystallographic data are summarized in Table 1, and selected bond distances with their estimated standard deviations are given in Table 2. As given in Table 1, three compounds are isomorphic to each other. The structure of $[\{Cu^{II}LGd^{III}(o\text{-van})(CH_3COO)(MeOH)\}_2]\cdot 2H_2O$ is described in detail. Figure 1 shows a cyclic $Cu^{II}{}_2Gd^{III}{}_2$ tetranuclear structure, in which the tetranuclear molecule has an inversion center and the Cu^{II} component functions as a "bridging ligand-complex" between two adjacent Gd^{III} ions. The coordination geometry of the Cu^{II} ion can essentially be described as square planar determined by the N_2O_2 donor atoms of the tetradentate ligand, while it should be noted that a methanol

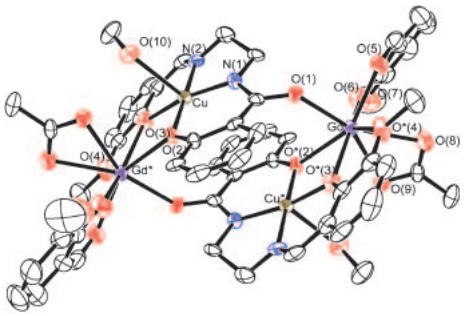

Fig. 1. Molecular structure of cyclic tetranuclear complex $[\{Cu^{II}LGd^{III}(o\text{-van})(CH_3COO)(MeOH)\}_2]\cdot 2H_2O$ with 30% thermal probability ellipsoids and selected atom labeling scheme. The hydrogen atoms were omitted for clarity.

molecule weakly coordinates to Cu^{II} ion at the fifth axial site, judging from the distance Cu–O(10) = 2.515(5) Å. The Cu–N(1) = 1.917(5) Å and Cu–O(2) = 1.922(4) Å distances of the 2-oxybenzamido moiety are considerably shorter than the corresponding values of the 2-oxy-3-methoxybenzaldehyde moiety (Cu–N(2) = 1.950(6) Å, Cu–O(3) = 1.948(4) Å), whose structural properties are also found in $[\{Cu^{II}LGd^{III}(hfac)_2\}_2]$.[13] The two phenolato (O(2) and O(3)) and the methoxy (O(4)) oxygen atoms on one side of the Cu^{II} complex coordinate to a Gd^{III} ion as a tridentate ligand: Gd*–O(2) = 2.430(4) Å, Gd*–O(3) = 2.367(4) Å, Gd*–O(4) = 2.580(4) Å, and Cu···Gd* = 3.4138(8) Å. The amido oxygen atom (O(1)) on the opposite side of the Cu^{II} complex coordinates to the other Gd^{III} ion as a monodentate ligand with Gd–O(1) = 2.280(5) Å and Cu···Gd = 5.7342(7) Å. One *o*-vanillin and one acetate ion coordinate to Gd^{III} ion, both as a bidentate ligand. Including one bidentate *o*-vanillin (Gd–O = 2.283(6)–2.398(5) Å) and one acetate ion (Gd–O = 2.441(5)–2.470(4) Å), which is a bidentate ligand, the Gd^{III} ion has a nonacoordinate geometry with nine oxygen atoms, O_9. It should be noted that the Gd–O bond distance with the amido oxygen (Gd–O(1) = 2.280(5) Å) is the shortest among the nine Gd–O bond distances. In the cyclic structure, there is no bridging ligand between the two Cu^{II} ions and between the two Gd^{III} ions. The Cu···Cu* and Gd···Gd* distances are 5.2388(9) and 7.8502(4) Å, respectively, indicating that the tetranuclear complex can be considered as a dimer of dimers and that the metal ions within each pair are strongly coupled. Cyclic tetranuclear molecules are well separated each other and the compound can be described as consisting of isolated molecules.

Dc Magnetic Properties of $[\{Cu^{II}LLn^{III}(o\text{-van})(CH_3COO)(MeOH)\}_2]\cdot 2H_2O$ (Ln^{III} = Gd^{III}, Tb^{III}, and Dy^{III}). The temperature dependence of the magnetic susceptibilities in the temperature range 2.0–300.0 K under the external magnetic field of 0.5 T for three complexes is shown in Fig. 2, as the plots of $\chi_M T$ vs T and $1/\chi_M$ vs T. The field dependence of the magnetization up to 5 T at 2.0 K is shown in Fig. 3, as the plots of $M/N\beta$ vs H.

$[\{Cu^{II}LGd^{III}(o\text{-van})(CH_3COO)(MeOH)\}_2]\cdot 2H_2O$: The $\chi_M T$ value of 16.14 $cm^3\,K\,mol^{-1}$ at 300.0 K is consistent with the theoretical value of 16.51 $cm^3\,K\,mol^{-1}$ expected for two Cu^{II} ($S = 1/2$) and two Gd^{III} ($4f^7$, $J = 7/2$, $L = 0$, $S = 7/2$, $^8S_{7/2}$) non-interacting ions, using the equation $\chi_M = 2\chi_{3d} + 2\chi_{4f}$ where $\chi_{3d} = (Ng^2\beta^2/3kT)[S(S+1)]$ and $\chi_{4f} = (Ng_J{}^2\beta^2/3kT)[J(J+1)]$, $g_J = 3/2 + [S(S+1) - L(L+1)]/2J(J+1)$.[14] On lowering the temperature, the $\chi_M T$ value increased gradually to reach a maximum of 25.51 $cm^3\,K\,mol^{-1}$ at 4.0 K and then decreased. The increase in the higher-temperature region indicates that there are ferromagnetic interactions between Cu^{II} and Gd^{III} ions while the decrease in the lower-temperature region is ascribed to a weak intra- and/or inter-molecular antiferromagnetic interaction. The reciprocal magnetic susceptibilities in the temperature range of 50–300 K follow the Curie–Weiss equation $1/\chi_M = (T-\theta)/C$ with $C = 15.78$ $cm^3\,K\,mol^{-1}$ and $\theta = +7.9$ K. Since the ground state of the Gd^{III} ion ($^8S_{7/2}$) had no contribution from orbital angular mo-

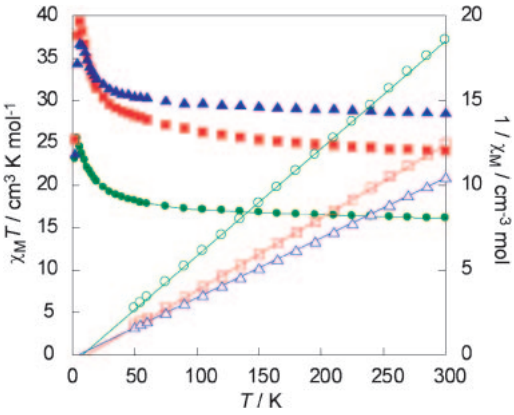

Fig. 2. Plots of $\chi_M T$ vs T and $1/\chi_M$ vs T for $[\{Cu^{II}LLn^{III}(o\text{-van})(CH_3COO)(MeOH)\}_2]\cdot 2H_2O$ (Ln^{III} = Gd^{III} (●), Tb^{III} (■), and Dy^{III} (▲)). The reciprocal magnetic susceptibilities in the temperature range 50–300 K (open circle, square, and triangle) were fitted to $1/\chi_M = (T-\theta)/C$ and the evaluated parameters are given in the text. The solid green line in the $\chi_M T$ vs T plot for $[\{Cu^{II}LGd^{III}(o\text{-van})(CH_3COO)(MeOH)\}_2]\cdot 2H_2O$ represents the theoretical curve with the best-fit parameters of $g = 1.97$, $J_1 = +3.8\,cm^{-1}$, $J_2 = +0.7\,cm^{-1}$, and $zJ' = -0.01\,cm^{-1}$.

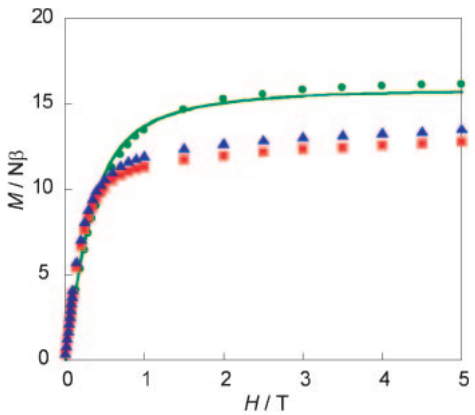

Fig. 3. Field dependence of the magnetization of $[\{Cu^{II}LLn^{III}(o\text{-van})(CH_3COO)(MeOH)\}_2]\cdot 2H_2O$ (Ln^{III} = Gd^{III} (●), Tb^{III} (■), and Dy^{III} (▲)) at 2.0 K. The solid line of $[\{Cu^{II}LGd^{III}(o\text{-van})(CH_3COO)(MeOH)\}_2]\cdot 2H_2O$ represents the theoretical curve of the Brillouin function with $g = 1.97$ and $S = 8$ spin ground state produced by the Cu^{II}–Gd^{III} ferromagnetic coupling of the spin system (1/2, 7/2, 1/2, and 7/2) with a cyclic structure.

mentum, the magnetic susceptibility of the $Cu^{II}_2Gd^{III}_2$ complex could be reproduced by the equation derived from the spin-only Hamiltonian $\boldsymbol{H} = g\beta(S_{Cu1} + S_{Cu2} + S_{Gd1} + S_{Gd2})\cdot H - 2J_1(S_{Cu1}S_{Gd1} + S_{Cu2}S_{Gd2}) - 2J_2(S_{Cu1}S_{Gd2} + S_{Cu2}S_{Gd1})$ based on a cyclic tetranuclear structure, where a common g-factor for the Gd^{III} and Cu^{II} ions was used, H is the applied magnetic field, J_1 and J_2 are the Heisenberg coupling constants between Cu^{II} and Gd^{III} ions for the two different magnetic paths and the intramolecular Cu^{II}–Cu^{II} and Gd^{III}–Gd^{III} magnetic interactions were neglected due to the lack of any magnetic paths. The magnetic susceptibility at each temperature was calculated using the theoretical equation $\chi = M/H = [N\sum_i(-dE_i/dH)\exp(-E_i/kT)]/[H\sum_i \exp(-E_i/kT)$. The energy levels of the tetramer, E_i, were evaluated by diagonalizing the Hamiltonian matrix (with dimensions 256×256) using an uncoupled spin function basis set. Moreover, a molecular field term $-zJ'\langle S_z\rangle S_z$ was added to the Hamiltonian to describe the molecular interactions between the tetrameric units. Although small, these interactions are necessary to reproduce the decrease of the magnetic moment below 4 K. The final expression for the magnetic susceptibility becomes, $\chi_{mf} = \chi/[1 - zJ'\chi/Ng^2\beta^2]$, where χ is the magnetic susceptibility for the isolated tetramer, calculated as described above. The solid line in Fig. 2 shows the theoretical curve with the best-fit parameters of $g = 1.97$, $J_1 = +3.8\,cm^{-1}$, $J_2 = +0.7\,cm^{-1}$, and $zJ' = -0.01\,cm^{-1}$, demonstrating that ferromagnetic interactions occur between Cu^{II} and Gd^{III} ions both through the amido bridge and the di-μ-phenolato bridge. Ferromagnetic coupling between Cu^{II} and Gd^{III} ions has been found in a number of $[Cu^{II}_nGd^{III}_m]$ polynuclear complexes,[15] and the present coupling constants are in the range of those previously reported.[15] As shown in the solid line of Fig. 3, the field dependence of the magnetization at 2.0 K was well reproduced by using the Brillouin function for an $S = 8$ spin ground state resulting from the Cu^{II}–Gd^{III} ferromagnetic coupling within the cyclic $Cu^{II}_2Gd^{III}_2$ tetramer using the $g = 1.97$. Therefore, the curve fitting of the magnetization as well as that of the magnetic susceptibility indicates that tetranuclear compound has a $S = 8$ spin ground state resulting from the Cu^{II}–Gd^{III} ferromagnetic coupling within the cyclic $Cu^{II}_2Gd^{III}_2$ tetramer.

[{Cu^{II}LTb^{III}(*o*-van)(CH$_3$COO)(MeOH)}$_2$]·2H$_2$O: The reciprocal magnetic susceptibilities in the temperature range 50–300 K follow $1/\chi_M = (T - \theta)/C$ with $C = 23.30\,cm^3\,K\,mol^{-1}$ and $\theta = +11.0$ K. The χ_MT value of 24.05 $cm^3\,K\,mol^{-1}$ at 300.0 K and C value are consistent with the value of 24.39 $cm^3\,K\,mol^{-1}$ expected for two Cu^{II} ($S = 1/2$) and two Tb^{III} ($4f^8$, $J = 6$, $S = 3$, $L = 3$, $^7F_6$) magnetically isolated ions. On lowering the temperature, the χ_MT value increased gradually to reach a maximum value of 39.29 $cm^3\,K\,mol^{-1}$ at 6.0 K and then decreased abruptly. The increase in the higher-temperature region and the positive θ value indicate there are ferromagnetic interaction between the Cu^{II} and Tb^{III} ions. As shown in Fig. 3, upon increasing the applied external magnetic field, the magnetization increased to 12.76 $N\beta$ at 5 T but did not reach the expected saturation value of 20 $N\beta$ (9 $N\beta$ for each Tb^{III} ion). This is due to the crystal field effect on the Tb^{III} ion ($4f^8$, $J = 6$, $S = 3$, $L = 3$, $^7F_6$) that removes the 13-fold degeneracy of the $^7F_6$ ground state.

[{Cu^{II}LDy^{III}(*o*-van)(CH$_3$COO)(MeOH)}$_2$]·2H$_2$O: The reciprocal magnetic susceptibilities in the temperature range 50–300 K follow $1/\chi_M = (T - \theta)/C$ with a $C = 28.28\,cm^3\,K\,mol^{-1}$ and $\theta = +4.8$ K. The C value and the χ_MT value at 300.0 K of 28.64 $cm^3\,K\,mol^{-1}$ are consistent with the value of 29.09 $cm^3\,K\,mol^{-1}$ expected for two Cu^{II} ($S = 1/2$) and two Dy^{III} ($4f^9$, $J = 15/2$, $S = 5/2$, $L = 5$, $^6H_{15/2}$) magnetically isolated ions. On lowering the temperature, the χ_MT value slightly increased to reach a maximum value of 36.79 $cm^3\,K\,mol^{-1}$ at 6.0 K, and then decreased abruptly. The increase in the higher-temperature region and the positive θ indicate that there are ferromagnetic interactions between the Cu^{II} and Dy^{III} ions. Upon increasing the applied external magnetic field, the magnetization increased to over 13.54 $N\beta$ at 5 T, but did not reach the expected saturation value of 22 $N\beta$ (10 $N\beta$ per each Dy^{III} ion). This is again due to crystal field effects on the Dy^{III} ion, which remove the 16-fold degeneracy of the $^6H_{15/2}$ ground state.

Ac Magnetic Properties. Since one of the characteristics of a SMM is the observation of an out-of-phase (χ_M'') ac susceptibility signal, temperature-dependent ac magnetic measurements for [{Cu^{II}LLn^{III}(*o*-van)(CH$_3$COO)(MeOH)}$_2$]·2H$_2$O (Ln^{III} = Tb^{III} and Dy^{III}) were carried out in a 3.0 G ac field oscillating at the indicated frequencies (1–1000 Hz) and with a zero dc field, where the lowest temperature is 1.8 K. Ac measurements for [{Cu^{II}LGd^{III}(*o*-van)(CH$_3$COO)(MeOH)}$_2$]·2H$_2$O were not performed, since the similar tetranuclear complex [{Cu^{II}L′Gd^{III}(hfac)$_2$}$_2$] (L′ is the 1:1:1 condensation product of *o*-vanillin, 1,2-*trans*-cyclohexanediamine, and 2-hydroxybenzamide) did not show frequency dependence, demonstrating that the magnetic anisotropy from the f-element is essential for SMMs behavior within the cyclic tetranuclear 3d–4f framework.

Ac Magnetic Susceptibility of [{Cu^{II}LTb^{III}(*o*-van)(CH$_3$COO)(MeOH)}$_2$]·2H$_2$O: Figure 4 shows the plots of the in-phase (χ_M') signal as $\chi_M'T$ and χ_M'' vs temperature (T). $\chi_M'T$ signal showed a frequency dependent decrease at $T < 4$ K, indicative of the onset of slow relaxation on the millisecond timescale, which is a diagnostic of a SMM. This was confirmed by the appearance of an out-of-phase signal due to the inability to relax rapidly enough at these temperatures to keep up with the oscillating field. The χ_M'' signal has a peak at 2.6 K at a 1000 Hz ac frequency, where the position of the peak corresponds to the temperature at which the relaxation rate is equal to the ac oscillation frequency. Data obtained by varying the frequency of oscillation of the ac field was fit to the Arrhenius equation ($\tau = \tau_0\exp(-\Delta/kT)$; $\tau = 1/2\pi\nu_{Max}$) to obtain the energy barrier for the relaxation of the magnetization, where τ, τ_0, Δ, and k denote relaxation time, preexponential factor, activation energy, and Boltzmann's constant, respectively. Figure 5 shows the Arrhenius plots as $\ln\tau$ vs $1/T$, and the best fitting parameters obtained are $\tau_0 = 7.1 \times 10^{-8}$ s, $-\Delta/k = 20.4$ K, and $T_B = 1.24$ K.

Ac Magnetic Susceptibility of [{Cu^{II}LDy^{III}(*o*-van)(CH$_3$COO)(MeOH)}$_2$]·2H$_2$O: Figure 6 shows the result of ac magnetic susceptibilities. Frequency dependence of ac susceptibilities ($\chi_M'T$ and χ_M'') is indicative of slow relaxation of the magnetization and one of the characteristics of a SMM. As shown in Fig. 6, the χ_M'' vs T plots is not a single peak, and in addition to the peaks in the temperature region above

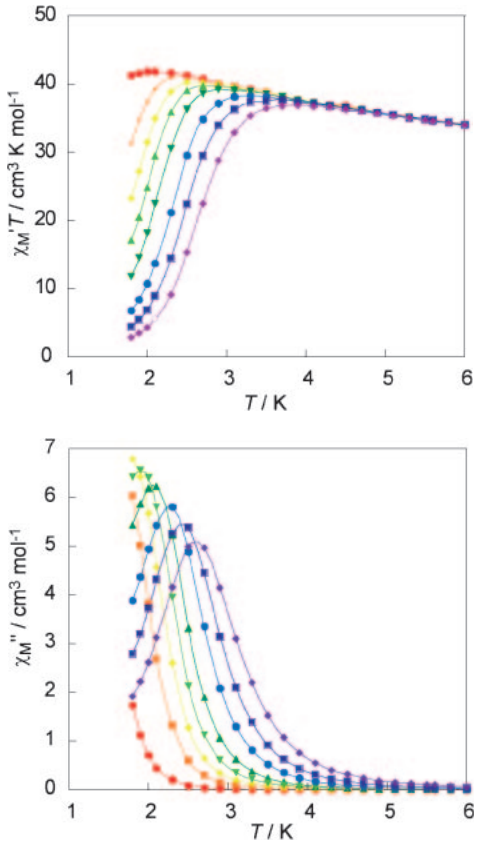

Fig. 4. Plots of $\chi_M'T$ vs T and χ_M'' vs T of [{$Cu^{II}LTb^{III}$-(o-van)(CH_3COO)(MeOH)}$_2$]·$2H_2O$, showing frequency dependence (1, 10, 25, 50, 100, 250, 500, and 1000 Hz).

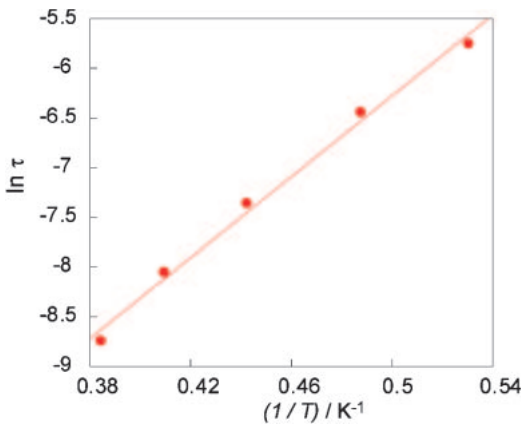

Fig. 5. Arrhenius plots of [{$Cu^{II}LTb^{III}$(o-van)(CH_3COO)-(MeOH)}$_2$]·$2H_2O$, as the plots of $\ln\tau$ vs $1/T$. The solid line represents a least-squares fit of the data to the Arrhenius equation ($\ln\tau = \ln\tau_0 - (\Delta/k)/T$).

1.8 K, the larger peak seems to appear at the lower temperature region. At the present stage, it is not clear whether these two peaks come from two species or from weak intermolecular magnetic interactions. Costes et al. have reported similar magnetic behavior in a 3d–4f complex with a similar teteranuclear framework and have demonstrated the weak intermolecular antiferromagnetic interactions are present on the basis of the hysteresis measurements.[7c]

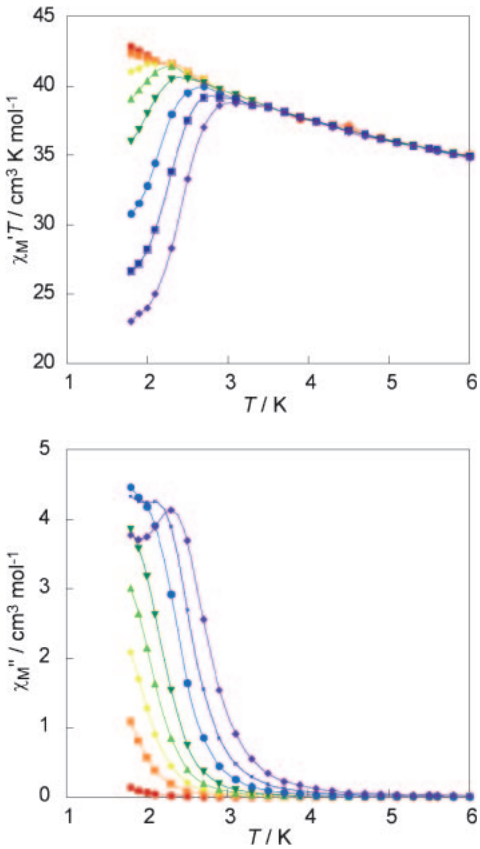

Fig. 6. Plots of $\chi_M'T$ vs T and χ_M'' vs T of [{$Cu^{II}LDy^{III}$-(o-van)(CH_3COO)(MeOH)}$_2$]·$2H_2O$, showing frequency dependence (1, 10, 25, 50, 100, 250, 500, and 1000 Hz).

Concluding Remarks

Three tetranuclear copper(II)–lanthanide(III) complexes, [{$Cu^{II}LLn^{III}$(o-van)(CH_3COO)(MeOH)}$_2$]·$2H_2O$ (Ln^{III} = Gd^{III}, Tb^{III}, and Dy^{III}), were synthesized and structurally and magnetically characterized. It was confirmed that the Cu^{II}_2–Tb^{III}_2 and Cu^{II}_2–Dy^{III}_2 clusters are SMMs with a cyclic tetranuclear structure. Several 3d–4f clusters have been reported to behave as SMMs, in which the complexes display frequency dependent χ_M'' signals,[3–9] and only a few compounds including our compounds show a maximum peak above 1.8 K.[5a,5b,8c] The parameters of the bistable energy barrier were evaluated from the Arrhenius equation: [$Mn^{III}_{11}Dy^{III}_4O_8(OH)_{10}(OMe)_2(O_2CPh)_{10}$-$(NO_3)_5(H_2O)$],[5a] $\tau_0 = 4 \times 10^{-8}$ s, $-\Delta/k = 9.3$ K; [NMe_4]$_2$-[$Mn^{III}_2Dy^{III}_2(tmp)_2(O_2CMe_3)_4(NO_3)_4$]·2MeCN·$0.5H_2O$,[5b] $\tau_0 = 3.31 \times 10^{-7}$ s, $-\Delta/k = 15$ K; {[$Dy(hfac)_{32}$]$_2$[$Cu(dpk)_2$]}[8c] (dpk = di-2-pyridyl ketooximate), $\tau_0 = 1.1 \times 10^{-7}$ s, $-\Delta/k =$ 47 K; [{$Cu^{II}LTb^{III}(hfac)_2$}$_2$],[4] $\tau_0 = 2.7 \times 10^{-8}$ s, $-\Delta/k = 21$ K; [{$Cu^{II}LTb^{III}$(o-van)(CH_3COO)(MeOH)}$_2$]·$2H_2O$, $\tau_0 =$ 7.1×10^{-8} s, $-\Delta/k = 20.4$ K. Our cyclic Cu^{II}_2–Tb^{III}_2 compounds [{$Cu^{II}LTb^{III}(hfac)_2$}$_2$] and [{$Cu^{II}LTb^{III}$(o-van)(CH_3-COO)(MeOH)}$_2$]·$2H_2O$, had similar energy barrier and blocking temperatures, suggesting that the ligand substitution of Tb^{III} component at the terminal sites produces no effective effort on these parameters. The complexes, [$Mn^{III}_{11}Dy^{III}_4O_8$-$(OH)_{10}(OMe)_2(O_2CPh)_{10}(NO_3)_5(H_2O)$],[5a] [$NMe_4$]$_2$[$Mn^{III}_2Dy^{III}_2$-$(tmp)_2(O_2CMe_3)_4(NO_3)_4$]·2MeCN·$0.5H_2O$,[5b] {[$Dy(hfac)_{32}$]$_2$-

$\{Cu(dpk)_2\}\}$,[8c] and $[\{Cu^{II}LTb^{III}(hfac)_2\}_2]$[16] were confirmed to display temperature and sweep rate dependent hysteresis loops by low-temperature magnetization studies, demonstrating that the molecular design of 3d–4f clusters is an effective and an alternative route to SMMs.

Experimental

Materials. All chemicals and solvents used for the synthesis were reagent grade and were obtained from Tokyo Kasei Co., Ltd and Wako Co., Ltd. and used without further purification. The copper(II) complex $K[Cu^{II}L]\cdot MeOH$ was prepared according to the method reported previously,[13] where the ligand H_3L is 1-(2-hydroxybenzamido)-2-(2-hydroxy-3-methoxybenzylideneamino)-ethane, obtained from the 1:1:1 condensation of *o*-vanillin (3-methoxysalicylaldehyde), ethylenediamine, and 2-hydroxybenzamide.

$[\{Cu^{II}LGd^{III}(o\text{-van})(CH_3COO)(MeOH)\}_2]\cdot 2H_2O$ (1). A methanolic solution (30 mL) of $K[Cu^{II}L]\cdot MeOH$ (81 mg, 0.18 mmol) was gently poured into a solution of $Gd(CH_3COO)_3\cdot 4H_2O$ (82 mg, 0.20 mmol) and *o*-vanillin (3-methoxysalicylaldehyde) (30 mg, 0.20 mmol) in a mixture of methanol (20 mL) and *N*,*N*′-dimethylformamide (5 mL) at ambient temperature. The resulting solution was allowed to stand for several days, during which time the dark reddish purple crystals precipitated were collected by suction filtration. The crystals were sparingly soluble even in *N*,*N*′-dimethylformamide (DMF) and the recrystallization could not be performed. Yield: 81%. IR (cm^{-1}, KBr pellet): $\nu_{C=O}$ 1634; $\nu_{C=N}$ 1603. Anal. Calcd for $C_{56}H_{62}Cu_2Gd_2N_4O_{22}$: C, 42.44; H, 3.94; N, 3.54%. Found: C, 42.41; H, 3.88; N, 3.53%.

$[\{Cu^{II}LTb^{III}(o\text{-van})(CH_3COO)(MeOH)\}_2]\cdot 2H_2O$ (2). This complex was prepared by the same method as for **1**, using $Tb(CH_3COO)_3\cdot 4H_2O$ instead of $Gd(CH_3COO)_3\cdot 4H_2O$. Dark reddish purple crystals were obtained. Yield: 88%. IR (cm^{-1}, KBr pellet): $\nu_{C=O}$ 1635; $\nu_{C=N}$ 1603. Anal. Calcd for $C_{56}H_{62}Cu_2Tb_2N_4O_{22}$: C, 42.35; H, 3.94; N, 3.53%. Found: C, 42.79; H, 3.98; N, 3.71%.

$[\{Cu^{II}LDy^{III}(o\text{-van})(CH_3COO)(MeOH)\}_2]\cdot 2H_2O$ (3). This complex was prepared by the same method as for **1**, using $Dy(CH_3COO)_3\cdot 4H_2O$ instead of $Gd(CH_3COO)_3\cdot 4H_2O$. Dark reddish purple crystals were obtained. Yield: 83%. IR (cm^{-1}, KBr pellet): $\nu_{C=O}$ 1636; $\nu_{C=N}$ 1603. Anal. Calcd for $C_{56}H_{62}Cu_2Dy_2N_4O_{22}$: C, 42.16; H, 3.92; N, 3.51%. Found: C, 41.53; H, 4.05; N, 3.85%.

Physical Measurements. Elemental C, H, and N analyses were carried out at the Instrumental Analysis Center of Kumamoto University. Infrared spectra were recorded on a Nicolet Avatar 370 DTGS spectrometer using KBr disks. Temperature-dependent dc magnetic susceptibilities in the temperature range 2.0–300.0 K and field-dependent magnetization under an applied magnetic field from 0 to 5 T at 2.0 K were measured with an MPMS-5S SQUID susceptometer (Quantum Design, Inc.) at Kumamoto University. The calibrations were performed with palladium. Corrections for diamagnetism were applied using Pascal's constants. Ac magnetic measurements were carried out at University of Wroclaw in a 3.0 G ac field oscillating at indicated frequencies (1–1000 Hz) with an Quantum design MPMS-XL5.

X-ray Crystallography. The X-ray diffraction data were collected on a Rigaku RAXIS RAPID imaging plate diffractometer using graphite monochromated Mo Kα radiation ($\lambda = 0.71073$ Å). The data were corrected for Lorentz, polarization, and absorption effects. The structures were solved by direct methods and expanded using the Fourier technique. Hydrogen atoms were fixed at the calculated positions and refined using a riding model. All calculations were performed using the Crystal Structure crystallographic software package.[17,18] The atomic scattering factors and anomalous dispersion terms were taken from the standard compilation.[19] Crystallographic data in the CIF format have been deposited under the deposition numbers CCDC 294933–294935. Copies of the data can be obtained free of charge via http://www.ccdc.cam.ac.uk/conts/retrieving.html (or from the Cambridge Crystallographic Data Centre, 12, Union Road, Cambridge, CB2 1EZ, UK; Fax: +44 1223 336033; e-mail: deposit@ccdc.cam.ac.uk).

This work was supported in part by a Grant-in-Aid for Science Research (No. 16655023 and No. 16205010) from the Ministry of Education, Culture, Sports, Science and Technology, Japan and by the Polish Ministry of Science and Education (Grant No. 1T09A 12430).

References

1 a) R. Sessoli, D. Gatteschi, A. Caneschi, M. A. Novak, *Nature* **1993**, *365*, 141. b) D. Gatteschi, A. Caneschi, L. Pardi, R. Sessoli, *Science* **1994**, *265*, 1054. c) R. Sessoli, H. L. Tsai, A. R. Schake, S. Wang, J. B. Vincent, K. Folting, D. Gatteschi, G. Christou, D. N. Hendrickson, *J. Am. Chem. Soc.* **1993**, *115*, 1804. d) L. Thomas, F. Lionti, R. Ballou, D. Gatteschi, R. Sessoli, B. Barbara, *Nature* **1996**, *383*, 145. e) C. Cadiou, M. Murrie, C. Paulsen, V. Villar, W. Wernsdorfer, W. E. P. Winpenny, *Chem. Commun.* **2001**, 2666. f) M. P. Shores, J. J. Sokol, J. R. Long, *J. Am. Chem. Soc.* **2002**, *124*, 2279. g) C. Boskovic, E. K. Brechin, W. E. Streib, K. Folting, J. C. Bollinger, D. N. Hendrickson, G. Christou, *J. Am. Chem. Soc.* **2002**, *124*, 3725. h) S. Ritter, *Chem. Eng. News* **2004**, *82*, 29.

2 D. Gatteschi, R. Sessoli, *Angew. Chem., Int. Ed.* **2003**, *42*, 268, and references therein.

3 a) N. Ishikawa, M. Sugita, W. Wernsdorfer, *J. Am. Chem. Soc.* **2005**, *127*, 3650. b) N. Ishikawa, M. Sugita, N. Tanaka, T. Ishikawa, S. Koshihara, Y. Kaizu, *Inorg. Chem.* **2004**, *43*, 5498. c) M. Sugita, N. Ishikawa, T. Ishikawa, S.-y. Koshihara, Y. Kaizu, *Inorg. Chem.* **2006**, *45*, 1299.

4 S. Osa, T. Kido, N. Matsumoto, N. Re, A. Pochaba, J. Mrozinski, *J. Am. Chem. Soc.* **2004**, *126*, 420.

5 a) A. Mishra, W. Wernsdorfer, K. A. Abboud, G. Christou, *J. Am. Chem. Soc.* **2004**, *126*, 15648. b) A. Mishra, W. Wernsdorfer, S. Parsons, G. Christou, F. K. Brechin, *Chem. Commun.* **2005**, 2086.

6 C. M. Zaleski, E. C. Depperman, J. W. Kampf, M. L. Kirk, V. Pecoraro, *Angew. Chem., Int. Ed.* **2004**, *43*, 3912.

7 a) F. He, M.-L. Tong, X.-M. Chen, *Inorg. Chem.* **2005**, *44*, 8285. b) J.-P. Costes, F. Dahan, W. Wernsdorfer, *Inorg. Chem.* **2006**, *45*, 5. c) J.-P. Costes, M. Auchel, F. Dahan, V. Peyrou, S. Shova, W. Wernsdorfer, *Inorg. Chem.* **2006**, *45*, 1924.

8 a) S. Ueki, M. Sahlan, T. Ishida, T. Nogami, *Synth. Met.* **2005**, *154*, 217. b) F. Mori, T. Ishida, T. Nogami, *Polyhedron* **2005**, *24*, 2588. c) F. Mori, T. Nyui, T. Ishida, T. Nogami, K.-Y. Choi, H. Nojiri, *J. Am. Chem. Soc.* **2006**, *128*, 1440.

9 C. Aronica, G. Pilet, G. Chastanet, W. Wernsdorfer, J.-F. Jacquot, D. Luneau, *Angew. Chem., Int. Ed.* **2006**, *45*, 4659.

10 M. Ferbinteanu, T. Kajiwara, K.-Y. Choi, H. Nojiri, A. Nakamoto, N. Kojima, F. Cimpoesu, Y. Fujimura, S. Takaishi, M. Yamashita, *J. Am. Chem. Soc.* **2006**, *128*, 9008.

11 a) Y. Yamaguchi, Y. Sunatsuki, M. Kojima, H. Akashi, M. Tsuchimoto, N. Re, S. Osa, N. Matsumoto, *Chem. Commun.* **2004**, 1048. b) Private communication from Prof. M. Kojima.

12 a) J. Tang, I. Hewitt, N. T. Madhu, G. Chastanet, W. Wernsdorfer, C. E. Ansen, C. Benelli, R. Sessoli, A. K. Powell, *Angew. Chem., Int. Ed.* **2006**, *45*, 1729. b) K. Bernot, L. Bogani, A. Caneschi, D. Gatteschi, R. Sessoli, *J. Am. Chem. Soc.* **2006**, *128*, 7947. c) L. Bogani, C. Sangregorio, R. Sessoli, D. Gatteschi, *Angew. Chem., Int. Ed.* **2005**, *44*, 5817.

13 a) T. Kido, S. Nagasato, Y. Sunatsuki, N. Matsumoto, *Chem. Commun.* **2000**, 2113. b) T. Kido, Y. Ikuta, Y. Sunatsuki, Y. Ogawa, N. Matsumoto, N. Re, *Inorg. Chem.* **2003**, *42*, 398. c) Y. Sunatsuki, T. Matsuo, M. Nakamura, F. Kai, N. Matsumoto, J.-P. Tuchagues, *Bull. Chem. Soc. Jpn.* **1998**, *71*, 2611. d) S. Osa, Y. Sunatsuki, Y. Yamamoto, M. Nakamura, T. Shimamoto, N. Matsumoto, N. Re, *Inorg. Chem.* **2003**, *42*, 5507.

14 a) M. L. Kahn, C. Mathoniere, O. Kahn, *Inorg. Chem.* **1999**, *38*, 3692. b) O. Kahn, *Molecular Magnetism*, VCH, Weinheim, **1993**.

15 a) A. Bencini, C. Benelli, A. Caneschi, R. L. Carlin, A. Dei, A. D. Gatteschi, *J. Am. Chem. Soc.* **1985**, *107*, 8128. b) J.-P. Costes, F. Dahan, A. Dupuis, J.-P. Laurent, *Inorg. Chem.* **2000**, *39*, 169. c) J.-P. Costes, F. Dahan, A. Dupuis, *Inorg. Chem.* **2000**, *39*, 165. d) J.-P. Costes, F. Dahan, A. Dupuis, J.-P. Laurent, *Inorg. Chem.* **1997**, *36*, 3429. e) M. Sasaki, K. Manseki, H. Horiuchi, M. Kumagai, M. Sakamoto, H. Sakiyama, Y. Nishida, M. Sakai, Y. Sadaoka, M. Ohba, H. Okawa, *J. Chem. Soc., Dalton Trans.* **2000**, 259. f) Q. Y. Chen, Q. H. Luo, L. M. Zheng, Z. L. Wang, J. T. Chen, *Inorg. Chem.* **2002**, *41*, 605. g) D. Gatteschi, R. Sessoli, A. Cornia, *Chem. Commun.* **2000**, 725. h) S. Akine, T. Matsumoto, T. Taniguchi, T. Nabeshima, *Inorg. Chem.* **2005**, *44*, 3270. i) D. Gatteschi, R. Sessoli, A. Cornia, *Chem. Commun.* **2000**, 725. j) J.-P. Costes, F. Dahan, A. Dupuis, J.-P. Laurent, *Chem. Eur. J.* **1998**, *4*, 1616.

16 J.-L. Gallani, IPCMS-GMO, Strasbourg, France, private communication.

17 D. J. Watkin, C. K. Prout, J. R. Carruthers, P. W. Betteridge, *CRYSTALS Issue 10*, Chemical Crystallography Laboratory, Oxford, UK.

18 *CrystalStructure 3.6.0; Crystal Structure Analysis Package*, Rigaku and Rigaku/MSC, 9009 New Trails Dr The Woodland TX 77381 U.S.A., **2000–2004**.

19 D. T. Cromer, J. T. Waber, *International Tables for X-ray Crystallography*, The Kynoch Press, Birmingham, England, **1974**, Vol. IV, Table 2.2 A.